

One-step implementation of a hybrid Fredkin gate with quantum memories and single superconducting qubit in circuit QED and its applications

TONG LIU, BAO-QING GUO, CHANG-SHUI YU,* AND WEI-NING ZHANG

School of Physics, Dalian University of Technology, Dalian 116024, China

*ycs@dlut.edu.cn

Abstract: In a recent remarkable experiment [R. B. Patel *et al.*, *Science advances* **2**, e1501531 (2016)], a 3-qubit quantum Fredkin (i.e., controlled-SWAP) gate was demonstrated by using linear optics. Here we propose a simple experimental scheme by utilizing the dispersive interaction in superconducting quantum circuit to implement a hybrid Fredkin gate with a superconducting flux qubit as the control qubit and two separated quantum memories as the target qubits. The quantum memories considered here are prepared by the superconducting coplanar waveguide resonators or nitrogen-vacancy center ensembles. In particular, it is shown that this Fredkin gate can be realized using a single-step operation and more importantly, each target qubit can be in an arbitrary state with arbitrary degrees of freedom. Furthermore, we show that this experimental scheme has many potential applications in quantum computation and quantum information processing such as generating arbitrary entangled states (discrete-variable states or continuous-variable states) of the two memories, measuring the fidelity and the entanglement between the two memories. With state-of-the-art circuit QED technology, the numerical simulation is performed to demonstrate that two-memory NOON states, entangled coherent states, and entangled cat states can be efficiently synthesized.

© 2024 Optical Society of America

OCIS codes: (270.0270) Quantum optics; (270.5585) Quantum information and processing; (020.5580) Quantum electrodynamics.

References and links

1. E. Fredkin and T. Toffoli, "Conservative logic", *Int. J. Theor. Phys.* **21**, 219-253 (1982).
2. I. L. Chuang and Y. Yamamoto, "Quantum bit regeneration", *Phys. Rev. Lett.* **76**, 4281 (1996).
3. D. G. Cory, M. D. Price, W. Maas, E. Knill, R. Laflamme, W. H. Zurek, T. F. Havel, and S. S. Somaroo, "Experimental quantum error correction", *Phys. Rev. Lett.* **81**, 2152 (1998).
4. H. F. Hofmann, "Weak values emerge in joint measurements on cloned quantum systems", *Phys. Rev. Lett.* **109**, 020408 (2012).
5. H. Buhrman, R. Cleve, J. Watrous, and R. de Wolf, "Quantum fingerprinting", *Phys. Rev. Lett.* **87**, 167902 (2001).
6. R. T. Horn, S. A. Babichev, K. P. Marzlin, A. I. Lvovsky, and B. C. Sanders, "Single-qubit optical quantum fingerprinting", *Phys. Rev. Lett.* **95**, 150502 (2005).
7. D. Gottesman and I. Chuang, "Quantum digital signatures", <https://arxiv.org/abs/quant-ph/0105032>.
8. H. F. Chau and F. Wilczek, "Simple realization of the Fredkin gate using a series of two-body operators", *Phys. Rev. Lett.* **75**, 748 (1995).
9. J. A. Smolin and D. P. DiVincenzo, "Five two-bit quantum gates are sufficient to implement the quantum Fredkin gate", *Phys. Rev. A* **53**, 2855 (1996).
10. Y. X. Gong, G. C. Guo, and T. C. Ralph, "Methods for a linear optical quantum Fredkin gate", *Phys. Rev. A* **78**, 012305 (2008).
11. R. B. Patel, J. Ho, F. Ferreyrol, T. C. Ralph, and G. J. Pryde, "A quantum Fredkin gate", *Science advances* **2**, e1501531 (2016).
12. A. Blais, R. S. Huang, A. Wallraff, S. M. Girvin, and R. J. Schoelkopf, "Cavity quantum electrodynamics for superconducting electrical circuits: an architecture for quantum computation", *Phys. Rev. A* **69**, 062320 (2004).
13. J. Clarke and F. K. Wilhelm, "Superconducting quantum bits", *Nature* **453**, 1031-1042 (2008).
14. J. Q. You and F. Nori, "Atomic physics and quantum optics using superconducting circuits", *Nature* **474**, 589-597 (2011).
15. G. Wendin, "Quantum information processing with superconducting circuits: a review", *Rep. Prog. Phys.* **80**, 106001 (2017).

16. A. Wallraff, D. I. Schuster, A. Blais, L. Frunzio, R. S. Huang, J. Majer, S. Kumar, S. M. Girvin, and R. J. Schoelkopf, "Strong coupling of a single photon to a superconducting qubit using circuit quantum electrodynamics", *Nature* **431**, 162-167 (2004).
17. I. Chiorescu, P. Bertet, K. Semba, Y. Nakamura, C. J. P. M. Harmans, and J. E. Mooij, "Coherent dynamics of a flux qubit coupled to a harmonic oscillator", *Nature* **431**, 159-162 (2004).
18. T. Niemczyk, F. Deppe, H. Huebl, E. P. Menzel, F. Hocke, M. J. Schwarz, J. J. Garcia-Ripoll, D. Zueco, T. Hümmer, E. Solano, A. Marx, and R. Gross, "Circuit quantum electrodynamics in the ultrastrong-coupling regime", *Nat. Physics* **6**, 772-776 (2010).
19. P. Forn-Díaz, J. Lisenfeld, D. Marcos, J. J. García-Ripoll, E. Solano, C. J. P. M. Harmans, and J. E. Mooij, "Observation of the Bloch-Siegert shift in a qubit-oscillator system in the ultrastrong coupling regime", *Phys. Rev. Lett.* **105**, 237001 (2010).
20. F. Yoshihara, T. Fuse, S. Ashhab, K. Kakuyanagi, S. Saito, and K. Semba, "Superconducting qubit-oscillator circuit beyond the ultrastrong-coupling regime", *Nat. physics* **13**, 44-47 (2017).
21. R. Amsüss, Ch. Koller, T. Nöbauer, S. Putz, S. Rotter, K. Sandner, S. Schneider, M. Schramböck, G. Steinhauser, H. Ritsch, J. Schmiedmayer, and J. Majer, "Cavity QED with magnetically coupled collective spin states", *Phys. Rev. Lett.* **107**, 060502 (2011).
22. Y. Kubo, C. Grezes, A. Dewes, T. Umeda, J. Isoya, H. Sumiya, N. Morishita, H. Abe, S. Onoda, T. Ohshima, V. Jacques, A. Dréau, J. F. Roch, I. Diniz, A. Auffeves, D. Vion, D. Esteve, and P. Bertet, "Hybrid quantum circuit with a superconducting qubit coupled to a spin ensemble", *Phys. Rev. Lett.* **107**, 220501 (2011).
23. X. Zhu, S. Saito, A. Kemp, K. Kakuyanagi, S. Karimoto, H. Nakano, W. J. Munro, Y. Tokura, M. S. Everitt, K. Nemoto, M. Kasu, N. Mizuochi, and K. Semba, "Coherent coupling of a superconducting flux qubit to an electron spin ensemble in diamond", *Nature* **478**, 221-224 (2011).
24. C. Simon, M. Afzelius, J. Appel, A. Boyer de la Giroday, S. J. Dewhurst, N. Gisin, C. Y. Hu, F. Jelezko, S. Kröll, J. H. Müller, J. Nunn, E. S. Polzik, J. G. Rarity, H. De Riedmatten, W. Rosenfeld, A. J. Shields, N. Sköld, R. M. Stevenson, R. Thew, I. A. Walmsley, M. C. Weber, H. Weinfurter, J. Wrachtrup, and R. J. Young, "Quantum memories", *Eur. Phys. J. D* **58**, 1-22 (2010).
25. M. Mariantoni, H. Wang, T. Yamamoto, M. Neeley, Radoslaw C. Bialczak, Y. Chen, M. Lenander, E. Lucero, A. D. O'Connell, D. Sank, M. Weides, J. Wenner, Y. Yin, J. Zhao, A. N. Korotkov, A. N. Cleland, J. M. Martinis, "Implementing the quantum von Neumann architecture with superconducting circuits", *Science* **334**, 61-65 (2011).
26. M. Reagor, H. Paik, G. Catelani, L. Sun, C. Axline, E. Holland, I. M. Pop, N. A. Masluk, T. Brecht, L. Frunzio, M. H. Devoret, L. Glazman, and R. J. Schoelkopf, "Reaching 10 ms single photon lifetimes for superconducting aluminum cavities", *Appl. Phys. Lett.* **102**, 192604 (2013).
27. M. Reagor, W. Pfaff, C. Axline, R. W. Heeres, N. Ofek, K. Sliwa, E. Holland, C. Wang, J. Blumoff, K. Chou, M. J. Hatridge, L. Frunzio, M. H. Devoret, L. Jiang, and R. J. Schoelkopf, "Quantum memory with millisecond coherence in circuit QED", *Phys. Rev. B* **94**, 014506 (2016).
28. C. Axline, M. Reagor, R. Heeres, P. Reinhold, C. Wang, K. Shain, W. Pfaff, Y. Chu, L. Frunzio, and R. J. Schoelkopf, "An architecture for integrating planar and 3D cQED devices", *Appl. Phys. Lett.* **109**, 042601 (2016).
29. N. Bar-Gill, L. M. Pham, A. Jarmola, D. Budker, and R. L. Walsworth, "Solid-state electronic spin coherence time approaching one second", *Nat. Commun.* **4**, 1743 (2013).
30. M. Mariantoni, F. Deppe, A. Marx, R. Gross, F. K. Wilhelm, and E. Solano, "Two-resonator circuit quantum electrodynamics: A superconducting quantum switch", *Phys. Rev. B* **78**, 104508 (2008).
31. S. T. Merkel and F. K. Wilhelm, "Generation and detection of NOON states in superconducting circuits", *New J. Phys.* **12**, 093036 (2010).
32. C. P. Yang, Q. P. Su, S. B. Zheng, F. Nori, and S. Han, "Entangling two oscillators with arbitrary asymmetric initial states", *Phys. Rev. A* **95**, 052341 (2017).
33. Q. P. Su, C. P. Yang, and S. B. Zheng, "Fast and simple scheme for generating NOON states of photons in circuit QED", *Sci. Rep.* **4**, 3898 (2014).
34. S. L. Ma, Z. Li, A. P. Fang, P. B. Li, S. Y. Gao, and F. L. Li, "Controllable generation of two-mode-entangled states in two-resonator circuit QED with a single gap-tunable superconducting qubit", *Phys. Rev. A* **90**, 062342 (2014).
35. M. Hua, M. J. Tao, and F. G. Deng, "One-step implementation of entanglement generation on microwave photons in distant 1D superconducting resonators", <https://arxiv.org/abs/1508.00061>.
36. T. Liu, Y. Zhang, B. Q. Guo, C. S. Yu, and W. N. Zhang, "Circuit QED: cross-Kerr effect induced by a superconducting qutrit without classical pulses", *Quantum Inf. Process.* **16**, 209 (2017).
37. F. W. Strauch, K. Jacobs, and R. W. Simmonds, "Arbitrary control of entanglement between two superconducting resonators", *Phys. Rev. Lett.* **105**, 050501 (2010).
38. F. W. Strauch, D. Onyango, K. Jacobs, and R. W. Simmonds, "Entangled-state synthesis for superconducting resonators", *Phys. Rev. A* **85**, 022335 (2012).
39. R. Sharma and F. W. Strauch, "Quantum state synthesis of superconducting resonators", *Phys. Rev. A* **93**, 012342 (2016).
40. Y. J. Zhao, C. Q. Wang, X. B. Zhu, and Y. X. Liu, "Engineering entangled microwave photon states through multiphoton interactions between two cavity fields and a superconducting qubit", *Sci. Rep.* **6**, 23646 (2016).
41. W. L. Yang, Y. Hu, Z. Q. Yin, Z. J. Deng, and M. Feng, "Entanglement of nitrogen-vacancy-center ensembles using transmission line resonators and a superconducting phase qubit", *Phys. Rev. A* **83**, 022302 (2011).

42. Q. Chen, W. L. Yang, and M. Feng, “Controllable quantum state transfer and entanglement generation between distant nitrogen-vacancy-center ensembles coupled to superconducting flux qubits”, *Phys. Rev. A* **86**, 022327 (2012).
43. H. Wang, M. Mariantoni, R. C. Bialczak, M. Lenander, E. Lucero, M. Neeley, A. D. O’Connell, D. Sank, M. Weides, J. Wenner, T. Yamamoto, Y. Yin, J. Zhao, J. M. Martinis, and A. N. Cleland, “Deterministic entanglement of photons in two superconducting microwave resonators”, *Phys. Rev. Lett.* **106**, 060401 (2011).
44. C. Wang, Y. Y. Gao, P. Reinhold, R. W. Heeres, N. Ofek, K. Chou, C. Axline, M. Reagor, J. Blumoff, K. M. Sliwa, L. Frunzio, S. M. Girvin, L. Jiang, M. Mirrahimi, M. H. Devoret, and R. J. Schoelkopf, “A Schrödinger cat living in two boxes”, *Science* **352**, 1087-1091 (2016).
45. D. F. James and J. Jerke, “Effective Hamiltonian theory and its applications in quantum information”, *Can. J. Phys.* **85**, 625-632 (2007).
46. X. Q. Shao, T. Y. Zheng, and S. Zhang, “Fast synthesis of the Fredkin gate via quantum Zeno dynamics”, *Quantum Inf. Process.* **11**, 1797-1808 (2012).
47. S. B. Zheng, “Implementation of Toffoli gates with a single asymmetric Heisenberg XY interaction”, *Phys. Rev. A* **87**, 042318 (2013).
48. X. Q. Shao, T. Y. Zheng, X. L. Feng, C. H. Oh, and S. Zhang, “One-step implementation of the genuine Fredkin gate in high-Q coupled three-cavity arrays”, *J. Opt. Soc. Am. B* **31**, 697-703 (2014).
49. T. J. Wang and C. Wang, “Universal hybrid three-qubit quantum gates assisted by a nitrogen-vacancy center coupled with a whispering-gallery-mode microresonator”, *Phys. Rev. A* **90**, 052310 (2014).
50. L. C. Song, Y. Xia, and J. Song, “Experimentally optimized implementation of the Fredkin gate with atoms in cavity QED”, *Quantum Inf. Process.* **14**, 511-529 (2015).
51. H. R. Wei and G. L. Long, “Hybrid quantum gates between flying photon and diamond nitrogen-vacancy centers assisted by optical microcavities”, *Sci. Rep.* **5**, 12918 (2015).
52. B. C. Ren, G. Y. Wang, and F. G. Deng, “Universal hyperparallel hybrid photonic quantum gates with dipole-induced transparency in the weak-coupling regime”, *Phys. Rev. A* **91**, 032328 (2015).
53. A. Lenef and S. C. Rand, “Electronic structure of the N-V center in diamond: Theory”, *Phys. Rev. B* **53**, 13441 (1996).
54. N. B. Manson, J. P. Harrison, and M. J. Sellars, “Nitrogen-vacancy center in diamond: Model of the electronic structure and associated dynamics”, *Phys. Rev. B* **74**, 104303 (2006).
55. P. Neumann, R. Kolesov, V. Jacques, J. Beck, J. Tisler, A. Batalov, L. Rogers, N. B. Manson, G. Balasubramanian, F. Jelezko, and J. Wrachtrup, “Excited-state spectroscopy of single NV defects in diamond using optically detected magnetic resonance”, *New J. Phys.* **11**, 013017 (2009).
56. Z. L. Xiang, X. Y. Lü, T. F. Li, J. Q. You, and F. Nori, “Hybrid quantum circuit consisting of a superconducting flux qubit coupled to a spin ensemble and a transmission-line resonator”, *Phys. Rev. B* **87**, 144516 (2013).
57. T. Hümmer, G. M. Reuther, P. Hänggi, and D. Zueco, “Nonequilibrium phases in hybrid arrays with flux qubits and nitrogen-vacancy centers”, *Phys. Rev. A* **85**, 052320 (2012).
58. R. Horodecki, P. Horodecki, M. Horodecki, and K. Horodecki, “Quantum entanglement”, *Rev. Mod. Phys.* **81**, 865-942 (2009).
59. P. Kok, H. Lee, and J. P. Dowling, “Creation of large-photon-number path entanglement conditioned on photodetection”, *Phys. Rev. A* **65**, 052104 (2002).
60. A. N. Boto, P. Kok, D. S. Abrams, S. L. Braunstein, C. P. Williams, and J. P. Dowling, “Quantum interferometric optical lithography: exploiting entanglement to beat the diffraction limit”, *Phys. Rev. Lett.* **85**, 2733 (2000).
61. I. Afek, O. Ambar, and Y. Silberberg, “High-NOON states by mixing quantum and classical light”, *Science* **328**, 879-881 (2010).
62. P. van Loock, N. Lütkenhaus, W. J. Munro, and K. Nemoto, “Quantum repeaters using coherent-state communication”, *Phys. Rev. A* **78**, 062319 (2008).
63. S. J. van Enk and O. Hirota, “Entangled coherent states: Teleportation and decoherence”, *Phys. Rev. A* **64**, 022313 (2001).
64. F. Grosshans and P. Grangier, “Continuous variable quantum cryptography using coherent states”, *Phys. Rev. Lett.* **88**, 057902 (2002).
65. J. Joo, W. J. Munro, and T. P. Spiller, “Quantum metrology with entangled coherent states”, *Phys. Rev. Lett.* **107**, 083601 (2011).
66. Y. F. Huang, B. H. Liu, L. Peng, Y. H. Li, L. Li, C. F. Li, and G. C. Guo, “Experimental generation of an eight-photon Greenberger-Horne-Zeilinger state”, *Nat. Commun.* **2**, 546 (2011).
67. X. C. Yao, T. X. Wang, P. Xu, H. Lu, G. S. Pan, X. H. Bao, C. Z. Peng, C. Y. Lu, Y. A. Chen, and J. W. Pan, “Observation of eight-photon entanglement”, *Nat. Photonics* **6**, 225-228 (2012).
68. C. A. Sackett, D. Kielpinski, B. E. King, C. Langer, V. Meyer, C. J. Myatt, M. Rowe, Q. A. Turchette, W. M. Itano, D. J. Wineland, and C. Monroe, “Experimental entanglement of four particles”, *Nature* **404**, 256-259 (2000).
69. T. Monz, P. Schindler, J. T. Barreiro, M. Chwalla, D. Nigg, W. A. Coish, M. Harlander, W. Hänsel, M. Hennrich, and R. Blatt, “14-qubit entanglement: creation and coherence”, *Phys. Rev. Lett.* **106**, 130506 (2011).
70. A. Rauschenbeutel, G. Nogues, S. Osnaghi, P. Bertet, M. Brune, J. M. Raimond, and S. Haroche, “Step-by-step engineered multiparticle entanglement”, *Science* **288**, 2024-2028 (2000).
71. S. Osnaghi, P. Bertet, A. Auffèves, P. Maioli, M. Brune, J. M. Raimond, and S. Haroche, “Coherent control of an atomic collision in a cavity”, *Phys. Rev. Lett.* **87**, 037902 (2001).

72. P. Neumann, N. Mizuochi, F. Rempp, P. Hemmer, H. Watanabe, S. Yamasaki, V. Jacques, T. Gaebel, F. Jelezko, and J. Wrachtrup, "Multipartite entanglement among single spins in diamond", *Science* **320**, 1326-1329 (2008).
73. H. Bernien, B. Hensen, W. Pfaff, G. Koolstra, M. S. Blok, L. Robledo, T. H. Taminiau, M. Markham, D. J. Twitchen, L. Childress, and R. Hanson, "Heralded entanglement between solid-state qubits separated by three metres", *Nature* **497**, 86-90 (2013).
74. M. Neeley, R. C. Bialczak, M. Lenander, E. Lucero, M. Mariantoni, A. D. O'Connell, D. Sank, H. Wang, M. Weides, J. Wenner, Y. Yin, T. Yamamoto, A. N. Cleland, and J. M. Martinis, "Generation of three-qubit entangled states using superconducting phase qubits", *Nature* **467**, 570-573 (2010).
75. L. DiCarlo, M. D. Reed, L. Sun, B. R. Johnson, J. M. Chow, J. M. Gambetta, L. Frunzio, S. M. Girvin, M. H. Devoret, and R. J. Schoelkopf, "Preparation and measurement of three-qubit entanglement in a superconducting circuit", *Nature* **467**, 574-578 (2010).
76. C. Song, K. Xu, W. Liu, C. P. Yang, S. B. Zheng, H. Deng, Q. Xie, K. Huang, Q. Guo, L. Zhang, P. Zhang, D. Xu, D. Zheng, X. Zhu, H. Wang, Y. A. Chen, C. Y. Lu, S. Han, and J. W. Pan, "10-qubit entanglement and parallel logic operations with a superconducting circuit", *Phys. Rev. Lett.* **119**, 180511 (2017).
77. R. Filip, "Overlap and entanglement-witness measurements", *Phys. Rev. A* **65**, 062320 (2002).
78. G. K. Brennen, "An observable measure of entanglement for pure states of multi-qubit systems", *Quantum Inf. Comput.* **3**, 619-626 (2003).
79. P. Horodecki, "Measuring Quantum Entanglement without Prior State Reconstruction", *Phys. Rev. Lett.* **90**, 167901 (2003).
80. C. S. Yu, J. Zhang, and H. Fan, "Quantum dissonance is rejected in an overlap measurement scheme", *Phys. Rev. A* **86**, 052317 (2012).
81. W. K. Wootters, "Entanglement of formation of an arbitrary state of two qubits", *Phys. Rev. Lett.* **80**, 2245 (1998).
82. M. Hofheinz, E. M. Weig, M. Ansmann, R. C. Bialczak, E. Lucero, M. Neeley, A. D. O'Connell, H. Wang, J. M. Martinis, and A. N. Cleland, "Generation of Fock states in a superconducting quantum circuit", *Nature* **454**, 310-314 (2008).
83. M. Hofheinz, H. Wang, M. Ansmann, R. C. Bialczak, E. Lucero, M. Neeley, A. D. O'Connell, D. Sank, J. Wenner, John M. Martinis, and A. N. Cleland, "Synthesizing arbitrary quantum states in a superconducting resonator", *Nature* **459**, 546-549 (2009).
84. B. Vlastakis, G. Kirchmair, Z. Leghtas, S. E. Nigg, L. Frunzio, S. M. Girvin, M. Mirrahimi, M. H. Devoret, R. J. Schoelkopf, "Deterministically encoding quantum information using 100-Photon Schrödinger cat states", *Science* **342**, 607-610 (2013).
85. R. W. Heeres, P. Reinhold, N. Ofek, L. Frunzio, L. Jiang, M. H. Devoret, and R. J. Schoelkopf, "Implementing a universal gate set on a logical qubit encoded in an oscillator", *Nat. Commun.* **8**, 94 (2017).
86. M. Baur, S. Filipp, R. Bianchetti, J. M. Fink, M. Göppl, L. Steffen, P. J. Leek, A. Blais, and A. Wallraff, "Measurement of Autler-Townes and Mollow transitions in a strongly driven superconducting qubit", *Phys. Rev. Lett.* **102**, 243602 (2009).
87. F. Yoshihara, Y. Nakamura, F. Yan, S. Gustavsson, J. Bylander, W. D. Oliver, and J. S. Tsai, "Flux qubit noise spectroscopy using Rabi oscillations under strong driving conditions", *Phys. Rev. B* **89**, 020503 (2014).
88. I. M. Pop, K. Geerlings, G. Catelani, R. J. Schoelkopf, L. I. Glazman, and M. H. Devore, "Coherent suppression of electromagnetic dissipation due to superconducting quasiparticles", *Nature* **508**, 369-372 (2014).
89. F. Yan, S. Gustavsson, A. Kamal, J. Birenbaum, A. P. Sears, D. Hover, T. J. Gudmundsen, D. Rosenberg, G. Samach, S. Weber, J. L. Yoder, T. P. Orlando, J. Clarke, A. J. Kerman, and W. D. Oliver, "The flux qubit revisited to enhance coherence and reproducibility", *Nature Comm.* **7**, 12964 (2016).
90. W. Chen, D. A. Bennett, V. Patel, and J. E. Lukens, "Substrate and process dependent losses in superconducting thin film resonators, Supercond", *Sci. Technol.* **21**, 075013 (2008).
91. P. J. Leek, M. Baur, J. M. Fink, R. Bianchetti, L. Steffen, S. Filipp, and A. Wallraff, "Cavity quantum electrodynamics with separate photon storage and qubit readout modes", *Phys. Rev. Lett.* **104**, 100504 (2010).

1. Introduction

The Fredkin gate is a three-qubit controlled-SWAP gate. Conditioned on the state of the control qubit, the gate can enable the two target qubits swap their quantum states [1]. It has played an important role in quantum computation and quantum information processing (QCQIP) such as error correction [2, 3], quantum cloning [4], quantum fingerprinting [5, 6], and quantum digital signatures [7]. Any multiqubit gate can in principle be decomposed into a sequence of single-qubit and two-qubit basic quantum gates, and there have been many proposals to implement the Fredkin gate which required at least six [8], five [9] and four [10] two-qubit gates. In particular, the Fredkin gate has been experimentally implemented with linear optics [11] on qubit systems. However, the multiqubit and even the high-dimensional quantum gates could be indispensable for the large scale quantum network and quantum processors. It is usually a significant challenge

to construct such multiqubit or high-dimensional quantum gates with the increase of the state space. The reason is mainly attributed to not only the experimental complications added but also the possibility of the errors caused by decoherence. Thus, it would be desirable to seek for efficient schemes based on a reliable physical platform to directly construct the Fredkin gate so as to reduce the operation time and experimental complications.

In analogy to cavity quantum electrodynamics (QED), the circuit QED system studying the light-matter interaction, is a specially suited platform to realize QCQIP due to its flexibility, scalability, and tunability [12–15]. The strong [16, 17], ultrastrong [18, 19], and beyond the ultrastrong coupling regimes [20] with a superconducting qubit coupled to a microwave resonator have been experimentally achieved in a series of experiments, and the strong coupling of an nitrogen-vacancy center ensemble (NV ensemble) to a superconducting resonator [21, 22] or flux qubit [23] has been experimentally realized in circuit QED. In addition, quantum memory is also indispensable in QCQIP such as quantum repeater and quantum computing [24]. A distinct feature of quantum memory is that it has the relatively large state space. In recent years, the solid-state devices (such as NV ensembles and superconducting resonators) have been considered as the good memory elements in QCQIP [24, 25]. Up to now, the superconducting resonator lifetimes between 1 and 10 ms have been reported [26–28] and a lifetime of 1 s for an NV ensemble has been experimentally achieved [29]. These experimental achievements directly lead to the further breakthrough in QCQIP. In particular, as the important physical resource, quantum entanglement in the context of circuit QED has attracted a great many of interest such as the preparation of a variety of entangled states (e.g., Bell states, NOON states, and entangled coherent states) of two superconducting resonators [30–40] or NV ensembles [41, 42]. Experimentally, the photon NOON states of two superconducting resonators have been produced [43], and a two-mode entangled coherent state of microwave fields in two superconducting resonators has been prepared [44]. Thus it is natural to consider how we can construct the Fredkin gate in high-dimensional systems by utilizing the well developed experimental technology in the superconducting quantum system.

Here, we propose a method for the *direct* realization of a general hybrid tripartite Fredkin gate by using superconducting resonators as two quantum memories coupled to a superconducting flux qubit. This gate can be expressed as

$$U(\gamma|g\rangle + \eta|e\rangle)|\psi\rangle_1|\varphi\rangle_2 = \gamma|g\rangle|\varphi\rangle_1|\psi\rangle_2 + \eta|e\rangle|\psi\rangle_1|\varphi\rangle_2, \quad (1)$$

where γ and η are the normalized complex numbers, $|\psi\rangle$ and $|\varphi\rangle$ are arbitrary pure states of target qudits encoded in two quantum memories 1 and 2, and $|g\rangle$ and $|e\rangle$ are the states of the control qubit. Eq. (1) shows that if and only if the control qubit is in the state $|g\rangle$, the two target qudits will swap their states, otherwise they remain in their initial states. Considering the experimental progress made in the NV center, we also propose an experimental scheme to realize the same aim as above by utilizing the NV ensembles as the quantum memories.

The two proposals have the following distinct advantages: (i) The Fredkin gate can be realized by employing a single unitary operation without need of any microwave pulse; (ii) Our method and experimental setup are simple because only a single qutrit and two target quantum memories are used; (iii) The experimental scheme is based on the superconducting resonator or the NV ensemble which has a long coherence time; (iv) Each controlled target qudit of this gate can be in an arbitrary state (*discrete-variable or continuous-variable state*) which can further lead to the wide applications such as (a) preparing an *arbitrary* entangled state of two superconducting resonators or NV ensembles, (b) directly measuring the fidelity between the two quantum memories as well as the entanglement between them without any information on the initial states required.

This paper is organized as follows. In Sec. 2, we explicitly show how to implement the hybrid Fredkin gate of a single superconducting flux qubit simultaneously controlling two target qudits

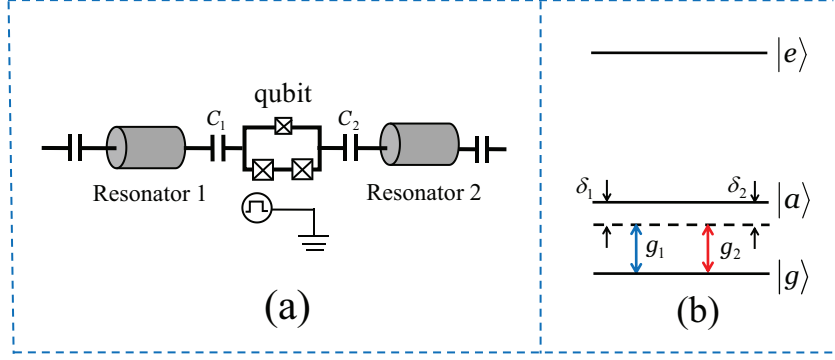


Fig. 1. (a) Setup of two superconducting resonators (i.e., 1 and 2) coupled to a flux qutrit (coupler) via capacitances C_1 and C_2 . (b) Resonator 1 (2) is far-off resonant with $|g\rangle \leftrightarrow |a\rangle$ transition of coupler with coupling strength g_1 (g_2) and detuning δ_1 (δ_2). Here, the detunings $\delta_1 = \omega_{ag} - \omega_{a_1}$ and $\delta_2 = \omega_{ag} - \omega_{a_2}$, the ω_{ag} is the $|g\rangle \leftrightarrow |a\rangle$ transition frequency of coupler and the ω_{a_1} (ω_{a_2}) is the frequency of resonator 1 (2).

encoded in two superconducting coplanar waveguide resonators or NV ensembles. In Sec. 3, we discuss the applications and the possible experimental implementation of our proposal and numerically calculate the operational fidelity for creating NOON states, entangled coherent states, and entangled cat states of two resonators or NV ensembles. A concluding summary is given in Sec. 4.

2. Hybrid Fredkin gate between a single superconducting qubit and two quantum memories

Superconducting resonators as quantum memories—We first consider such a system that consists of two superconducting microwave coplanar waveguide resonators coupled to a three-level superconducting flux qutrit (coupler) [Fig. 1(a)]. As shown in Fig. 1(b), the resonators 1 and 2 are off-resonantly coupled to the $|g\rangle \leftrightarrow |a\rangle$ transition of coupler with the coupling constants g_1 and g_2 , respectively. In the interaction picture, after making the rotating-wave approximation, the Hamiltonian of the whole system reads (in units of $\hbar = 1$)

$$H_{I,1} = g_1(e^{i\delta_1 t} a_1 \sigma_{ag}^+ + h.c.) + g_2(e^{i\delta_2 t} a_2 \sigma_{ag}^+ + h.c.), \quad (2)$$

where a_1 (a_2) is the photon annihilation operator for the resonator 1 (2), $\sigma_{ag}^+ = |a\rangle\langle g|$, $\delta_1 = \omega_{ag} - \omega_{a_1}$ and $\delta_2 = \omega_{ag} - \omega_{a_2}$. Here, ω_{ag} is the frequency of coupler related to the transition $|g\rangle \leftrightarrow |a\rangle$ and ω_{a_1} (ω_{a_2}) is the frequency of resonator 1 (2).

Considering the large-detuning conditions $\delta_1 \gg g_1$ and $\delta_2 \gg g_2$, the Hamiltonian (2) can be written as [45]

$$\begin{aligned} H_e = & \left(\frac{g_1^2}{\delta_1} a_1 a_1^\dagger + \frac{g_2^2}{\delta_2} a_2 a_2^\dagger \right) |a\rangle\langle a| - \left(\frac{g_1^2}{\delta_1} a_1^\dagger a_1 + \frac{g_2^2}{\delta_2} a_2^\dagger a_2 \right) |g\rangle\langle g| \\ & + \lambda (e^{i\delta' t} a_1^\dagger a_2 + e^{-i\delta' t} a_1 a_2^\dagger) |a\rangle\langle a| - \lambda (e^{-i\delta' t} a_1^\dagger a_2 + e^{i\delta' t} a_1 a_2^\dagger) |g\rangle\langle g|, \end{aligned} \quad (3)$$

where $\lambda = \frac{g_1 g_2}{2} \left(\frac{1}{\delta_1} + \frac{1}{\delta_2} \right)$ and $\delta' = \delta_2 - \delta_1$. The first line of Eq. (3) describes Stark shifts of the level $|a\rangle$ ($|g\rangle$) of the coupler; which the second line describes the interaction between the resonators 1 and 2 when the coupler is in the state $|a\rangle$ or $|g\rangle$.

For simplicity, we set

$$\delta_1 = \delta_2 = \delta, g_1 = g_2 = g, \quad (4)$$

and assume that the level $|a\rangle$ of coupler is not occupied. Thus, the effective Hamiltonian (3) is reduced to

$$H_e = H_0 + H_i \quad (5)$$

with

$$\begin{aligned} H_0 &= -\omega(a_1^\dagger a_1 + a_2^\dagger a_2)|g\rangle\langle g|, \\ H_i &= -\lambda(a_1^\dagger a_2 + a_1 a_2^\dagger)|g\rangle\langle g|, \end{aligned} \quad (6)$$

where $\omega = g_1^2/\delta_1 = g_2^2/\delta_2$. The Hamiltonian H_i describes the interaction between the resonators when the coupler is in the state $|g\rangle$.

Now we can show that the effective Hamiltonian (5) can be used to construct a hybrid Fredkin gate with the flux qubit simultaneously controlling the two target qudits encoded by two quantum memories. We suppose the quantum memory is prepared by a superconducting coplanar waveguide resonator or an NV ensemble. Let the initial state of the quantum memory 1 (2) be an arbitrary pure state $|\psi\rangle_1 = \sum_{n=0}^{\infty} c_n |n\rangle_1$ with $|n\rangle_1 = \frac{(a_1^\dagger)^n}{\sqrt{n!}}|0\rangle_1$ ($|\varphi\rangle_2 = \sum_{m=0}^{\infty} d_m |m\rangle_2$ with $|m\rangle_2 = \frac{(a_2^\dagger)^m}{\sqrt{m!}}|0\rangle_2$) and the flux qutrit be an arbitrary superposition state $|\phi\rangle_q = \gamma|g\rangle + \eta|e\rangle$. Note that only the two levels $|g\rangle$ and $|e\rangle$ of the flux qutrit are encoded here and will be used as the control qubit in the Fredkin gate. Here, c_n and d_m (γ and η) represent arbitrary complex amplitudes satisfying the normalization condition, $|0\rangle_1$ ($|0\rangle_2$) denotes the vacuum state of the quantum memory 1 (2). From Eq. (6), one can see that $[H_0, H_i] = 0$. Thus, the time-evolution operator for the Hamiltonian (5) can be defined as $U = e^{-iH_0 t} \cdot e^{-iH_i t}$. With the Hamiltonian (5), the state $|\phi\rangle_q |\psi\rangle_1 |\varphi\rangle_2$ of the qubit-memory system evolves into

$$\begin{aligned} U|\phi\rangle_q |\psi\rangle_1 |\varphi\rangle_2 &= e^{-iH_0 t} e^{-iH_i t} (\gamma|g\rangle + \eta|e\rangle) |\psi\rangle_1 |\varphi\rangle_2 \\ &= e^{i\omega(a_1^\dagger a_1 + a_2^\dagger a_2)t} |g\rangle\langle g| e^{i\lambda(a_1^\dagger a_2 + a_1 a_2^\dagger)t} |g\rangle\langle g| (\gamma|g\rangle + \eta|e\rangle) |\psi\rangle_1 |\varphi\rangle_2 \\ &= e^{i\omega(a_1^\dagger a_1 + a_2^\dagger a_2)t} e^{i\lambda(a_1^\dagger a_2 + a_1 a_2^\dagger)t} \gamma|g\rangle |\psi\rangle_1 |\varphi\rangle_2 + \eta|e\rangle |\psi\rangle_1 |\varphi\rangle_2 \\ &= e^{iH'_0 t} e^{iH'_i t} \gamma|g\rangle |\psi\rangle_1 |\varphi\rangle_2 + \eta|e\rangle |\psi\rangle_1 |\varphi\rangle_2, \end{aligned} \quad (7)$$

where $H'_0 = \omega(a_1^\dagger a_1 + a_2^\dagger a_2)$, $H'_i = \lambda(a_1^\dagger a_2 + a_1 a_2^\dagger)$, and $\langle g|e\rangle = 0$ has been used. It should be noted that the Hamiltonian H'_0 and H'_i are different from H_0 and H_i because the Hamiltonian H_0 and H_i contain a qubit operator $|g\rangle\langle g|$.

Making use of the Hamiltonian H'_i , one can obtain the transformations $e^{-iH'_i t} a_1^\dagger e^{iH'_i t} = \cos(\lambda t) a_1^\dagger - i \sin(\lambda t) a_2^\dagger$ and $e^{-iH'_i t} a_2^\dagger e^{iH'_i t} = \cos(\lambda t) a_2^\dagger - i \sin(\lambda t) a_1^\dagger$. For $\lambda t = \pi/2$, one has $e^{-iH'_i t} (a_1^\dagger)^n e^{iH'_i t} = (-i a_2^\dagger)^n$ and $e^{-iH'_i t} (a_2^\dagger)^m e^{iH'_i t} = (-i a_1^\dagger)^m$. After the evolution time $t = \pi/(2\lambda)$,

the Eq. (7) becomes

$$\begin{aligned}
& U|\phi\rangle_q|\psi\rangle_1|\varphi\rangle_2 \\
&= e^{iH'_0t} e^{iH'_1t} \gamma|g\rangle|\psi\rangle_1|\varphi\rangle_2 + \eta|e\rangle|\psi\rangle_1|\varphi\rangle_2 \\
&= e^{iH'_0t} \gamma|g\rangle \sum_{n=0}^{\infty} \sum_{m=0}^{\infty} \frac{c_n}{\sqrt{n!}} \frac{d_m}{\sqrt{m!}} e^{iH'_1t} (a_1^\dagger)^n (a_2^\dagger)^m |0\rangle_1 |0\rangle_2 + \eta|e\rangle|\psi\rangle_1|\varphi\rangle_2 \\
&= e^{iH'_0t} \gamma|g\rangle \sum_{n=0}^{\infty} \sum_{m=0}^{\infty} \frac{c_n}{\sqrt{n!}} \frac{d_m}{\sqrt{m!}} \left[e^{iH'_1t} (a_1^\dagger)^n e^{-iH'_1t} \right] \left[e^{iH'_1t} (a_2^\dagger)^m e^{-iH'_1t} \right] e^{iH'_1t} |0\rangle_1 |0\rangle_2 \\
&+ \eta|e\rangle|\psi\rangle_1|\varphi\rangle_2 \\
&= e^{iH'_0t} \gamma|g\rangle \sum_{m=0}^{\infty} \frac{d_m}{\sqrt{m!}} (-ia_1^\dagger)^m |0\rangle_1 \sum_{n=0}^{\infty} \frac{c_n}{\sqrt{n!}} (-ia_2^\dagger)^n |0\rangle_2 + \eta|e\rangle|\psi\rangle_1|\varphi\rangle_2 \\
&= \gamma|g\rangle|\varphi\rangle_1|\psi\rangle_2 + \eta|e\rangle|\psi\rangle_1|\varphi\rangle_2, \tag{8}
\end{aligned}$$

where we have used $a_1^\dagger a_1 |n\rangle = n (a_2^\dagger a_2 |m\rangle = m)$, $a_1 |0\rangle_1 = 0$ ($a_2 |0\rangle_2 = 0$), and $(-i)^n = e^{in\pi(2k-1/2)}$ ($(-i)^m = e^{im\pi(2k-1/2)}$) with k an integer. One finds that the phase factors $(-i)^n$ and $(-i)^m$ in Eq. (8) have been completely dropped for the evolution time $t = \pi/(2\lambda)$. Eq. (8) is a hybrid Fredkin gate which implies that iff the control qubit is in the state $|g\rangle$, the two target qubits swap their states but nothing otherwise.

We would like to mention that various schemes for achieving the three-qubit Fredkin gates have been previously suggested in [46–52], in which the two target qubits are encoded in two natural/artificial atoms [46–51] or photons [52]. Unlike the previous proposals, the target qubits of our gate are encoded in two superconducting resonators or NV ensembles which have the long coherence times. In contrast to [51] where the target qubits are encoded by the discrete-variable state, in our proposal the target qubits also can be encoded by the continuous-variable state. In addition, the proposals [46–52] require several operational steps and the microwave pulses, however, our proposal is much improved because our gate can be realized only using a single-step operation and no microwave pulses are needed.

NV ensembles as quantum memories— Now we would like to consider another system composing of a superconducting flux qubit coupled to two NV ensembles to realize the above Fredkin gate. The energy-level of an NV center consists of a ground state 3A , an excited state 3E and a metastable state 1A . Both 3A and 3E are spin triplet states while the metastable 1A is a spin singlet state [53, 54]. The NV center has an electronic spin triplet ground state with zero-field splitting $D_{gs}/(2\pi) \approx 2.878$ GHz between the $|m_s = 0\rangle$ and $|m_s = \pm 1\rangle$ levels. By applying an external magnetic field along the crystalline axis of the NV center [55, 56], an additional Zeeman splitting between $|m_s = \pm 1\rangle$ sublevels occurs [Fig. 2(a)].

We first consider a system consisting of a superconducting flux qubit coupled to an NV ensemble. The NV center is usually regarded as a spin while an NV ensemble is generally considered as a spin ensemble. We choose the $|g\rangle \leftrightarrow |a\rangle$ transition of qubit is coupled to the transition between the ground level $|m_s = 0\rangle$ and the excited level $|m_s = +1\rangle$ of the spins in the ensemble, but decoupled from the transition between the two levels $|m_s = 0\rangle$ and $|m_s = -1\rangle$. In the interaction picture, after making the rotating-wave approximation, the Hamiltonian of the flux qubit and the NV ensemble system is

$$H_{FN} = \sum_{k=1}^N \mu_k (\sigma_{ag}^+ \tau_k^- e^{i\Delta t} + \sigma_{ag}^- \tau_k^+ e^{-i\Delta t}), \tag{9}$$

where $\Delta = \omega_{ag} - \omega_{0,+1}$, $\tau_k^- = |m_s = 0\rangle_k \langle m_s = +1|$ and $\tau_k^+ = |m_s = +1\rangle_k \langle m_s = 0|$ are the lowering and raising operators of the k th spin, and μ_k is the coupling constant between the k th

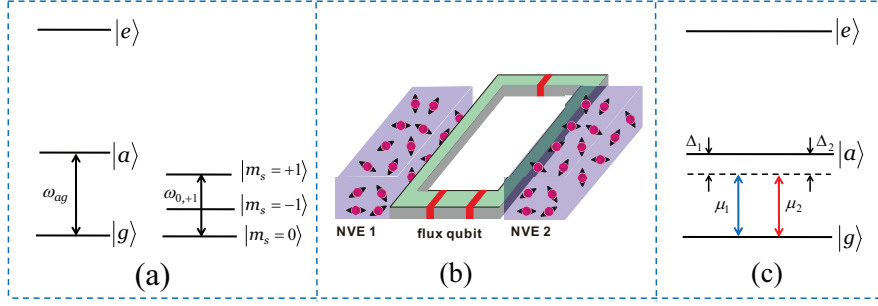


Fig. 2. (a) Energy level diagram of the flux and an NV center. By applying an external magnetic field along the crystalline axis of the NV center, an additional Zeeman splitting between $|m_s = \pm 1\rangle$ sublevels occurs. Here, ω_{ag} is the $|g\rangle \leftrightarrow |a\rangle$ transition frequency of flux qubit and $\omega_{0,+1}$ is the energy gap between the $|m_s = 0\rangle$ and $|m_s = +1\rangle$ levels of the NV center. (b) Illustration of the hybrid system consisted of a flux qubit and two NV ensembles. (c) The NV ensemble 1 (2) is far-off resonant with $|g\rangle \leftrightarrow |a\rangle$ transition of qubit with the coupling strength μ_1 (μ_2) and the detuning Δ_1 (Δ_2).

spin and the $|g\rangle \leftrightarrow |a\rangle$ transition of qubit. Here, $\omega_{0,+1}$ is the transition frequency between the two levels $|m_s = 0\rangle$ and $|m_s = +1\rangle$. We then introduce a collective operator

$$b^\dagger = \left(\frac{1}{\sqrt{N}} \right) \left(\frac{1}{\bar{\mu}} \right) \sum_{k=1}^N \mu_k \tau_k^+, \quad (10)$$

where $\bar{\mu}^2 = \sum_{k=1}^N |\mu_k|^2 / N$ with $\bar{\mu}$ the root mean square of the individual couplings.

Under the conditions of the large N and the low excitations, b^\dagger behaves as a bosonic operator and the spin ensemble behaves as a bosonic mode. Thus, one has $[b, b^\dagger] \approx 1$, and $b^\dagger b |n\rangle_b = n |n\rangle_b$ [56, 57], where $|n\rangle_b = \frac{1}{\sqrt{n!}} (b^\dagger)^n |0\rangle_b$ with $|0\rangle_b = |m_s = 0\rangle_1 |m_s = 0\rangle_2 \cdots |m_s = 0\rangle_N$. Accordingly, one has the frequency of the bosonic mode $\omega_b = \omega_{0,+1}$. Therefore, the Hamiltonian (9) can be further rewritten as

$$H_{FN} = \mu (e^{i\Delta t} b \sigma_{ag}^+ + e^{-i\Delta t} b^\dagger \sigma_{ag}^-), \quad (11)$$

with $\mu = \sqrt{N} \bar{\mu}$. We then consider a system consisting of a flux qubit coupled to two NV ensembles [Fig. 2(b)]. As depicted in Fig. 2(c), NV ensembles 1 and 2 are off-resonantly coupled to the $|g\rangle \leftrightarrow |a\rangle$ transition of qubit with coupling constants μ_1 and μ_2 , respectively. Based on Eq. (11), the Hamiltonian of the whole system is

$$H_{I,1} = \mu_1 (e^{i\Delta_1 t} b_1 \sigma_{ag}^+ + h.c.) + \mu_2 (e^{i\Delta_2 t} b_2 \sigma_{ag}^+ + h.c.), \quad (12)$$

where b_1 and b_2 are the corresponding annihilation operators for the NV ensembles 1 and 2, $\Delta_1 = \omega_{ag} - \omega_{b_1}$ and $\Delta_2 = \omega_{ag} - \omega_{b_2}$. Here, ω_{ag} is the $|g\rangle \leftrightarrow |a\rangle$ transition frequency of qubit and ω_{b_1} (ω_{b_2}) is the frequency of NV ensemble 1 (2).

Let's assume the large-detuning conditions $\Delta_1 \gg \mu_1$ and $\Delta_2 \gg \mu_2$ with (i) $\Delta_1 = \Delta_2$, $\mu_1 = \mu_2$, (ii) the level $|a\rangle$ of coupler qubit not occupied. One can find that the final effective Hamiltonian [for details, see Eqs. (3)-(5)] can be given by

$$H_e = H_0 + H_i \quad (13)$$

with

$$\begin{aligned} H_0 &= -\omega(b_1^\dagger b_1 + b_2^\dagger b_2)|g\rangle\langle g|, \\ H_i &= -\lambda(b_1^\dagger b_2 + b_1 b_2^\dagger)|g\rangle\langle g|, \end{aligned} \quad (14)$$

where $\omega = \mu_1^2/\Delta_1 = \mu_2^2/\Delta_2$ and $\lambda = \frac{\mu_1\mu_2}{2}(\frac{1}{\Delta_1} + \frac{1}{\Delta_2})$. When the qubit is in the state $|g\rangle$, the Hamiltonian H_i describes the interaction between the NV ensembles. It is obvious that the Hamiltonian Eq. (13) has the same form as Eq. (5), so the above demonstrated Fredkin gate can also be prepared with the NV ensembles as memories.

3. Applications and possible experimental implementation

The Fredkin gate has played a vital role and has many useful applications in QCQIP, such as error correction [2, 3], quantum cloning [4], quantum fingerprinting [5, 6], and quantum digital signatures [7]. In the following subsections, we will discuss some additional applications and the possible experimental implementation of our proposed Fredkin gate.

Preparation of entanglement—Entanglement as a physical phenomenon, is one of the most fundamental features of quantum mechanics [58]. Furthermore, entanglement is also an important physical resource to achieve many quantum information processing and communication tasks. For instance, the NOON states play the central role in quantum metrology [59], quantum optical lithography [60], and precision measurement [61]; the entangled coherent states can serve as an important resource for quantum networks [62], quantum teleportation [63], quantum cryptography [64], and quantum metrology [65]. Thus, the generation of entangled states is one of the key goals of QCQIP. Over the past two decades, many experiments have been reported for the generation of multiple-particle entangled states of photons [66, 67], ions [68, 69], natural atoms [70, 71], NV centers [72, 73], and superconducting qubits [74–76].

Our Fredkin gate can be used as an efficient quantum generator to produce the entanglement between two resonators or NV ensembles with the arbitrary (discrete variable or continuous variable) initial state. For example, we apply a microwave pulse to control qubit such that the pulse is resonant with the $|g\rangle \leftrightarrow |e\rangle$ transition of the control qubit. Making the rotating-wave approximation, the Hamiltonian in the interaction picture is written as $H_{I,2} = \Omega(e^{i\theta}|g\rangle\langle e| + h.c.)$, where Ω and θ are the Rabi frequency and the initial phase of the pulse. We choose $t' = \pi/(4\Omega)$ and $\theta = -\pi/2$ to pump the state $|e\rangle$ to $(|e\rangle - |g\rangle)/\sqrt{2}$ and $|g\rangle$ to $(|e\rangle + |g\rangle)/\sqrt{2}$. Accordingly, the state (8) changes to $\frac{1}{\sqrt{2}}(|\psi_+\rangle|e\rangle + |\psi_-\rangle|g\rangle)$, where $|\psi_\pm\rangle$ are the entangled states of two quantum memories, given by $|\psi_\pm\rangle = \gamma|\varphi\rangle_1|\psi\rangle_2 \pm \eta|\psi\rangle_1|\varphi\rangle_2$. Now if a von Neumann measurement is performed on flux qubit along a measurement basis $\{|g\rangle, |e\rangle\}$, one can see that the entangled state of two quantum memories is prepared in the $|\psi_+\rangle$ or $|\psi_-\rangle$. It should be noted here that $|\psi\rangle$ and $|\varphi\rangle$ are arbitrary nonsymmetric states.

The previous schemes for synthesizing an arbitrary two-resonator entangled state through two three-level superconducting qutrits coupled to three resonators assisted by a sequence of microwave pulses applied to the two qubits [31], or a four-level superconducting qudit [32] coupled to two resonators and driven by a microwave pulse. Compared with [31, 32], our experimental setup is greatly simplified and the experimental difficulty is reduced because only a single three-level qubit is employed and no microwave pulse is used. In addition, our proposal is based on a first-order large detuning, while the [32] was based on a second-order large detuning. This makes our operation faster than the one proposed by [32]. In recent years, several state-synthesis algorithms have been proposed to generate entangled states of two superconducting resonators [37–40]. These methods [37–40] depend on the maximum photon number and the number of operational steps required. While our proposal requires only a single unitary operation, which can significantly reduce the number of steps and the preparation time.

Measuring the fidelity and entanglement between the two quantum memories— Determining the overlap (or fidelity) of one quantum state with respect to another or the entanglement of a pure state based on the controlled-swap gate is a well-known method usually employed in qubit systems [77–80]. Here as an alternative demonstration in qudit systems, we will show that the above experimental scheme can also be used to determine the fidelity and entanglement between the two quantum memories. Let's consider such a scenario where the two quantum memories 1 and 2 are in a product state $|\psi\rangle_1 |\varphi\rangle_2$ and one wants to know whether $|\psi\rangle_1$ and $|\varphi\rangle_2$ are the same or not or to what degree they are different. To achieve this goal, one can first prepare the flux qubit in the state $|\phi\rangle_q = \gamma|g\rangle + \eta|e\rangle$ with the known parameter γ and η . Typically, we can set $\gamma = \eta = \frac{1}{\sqrt{2}}$. Let the tripartite quantum state $|\phi\rangle_q |\psi\rangle_1 |\varphi\rangle_2$ undergo the above preparation process of the entanglement, one can find that, before the final von Neumann measurement on the flux qubit, $|\phi\rangle_q |\psi\rangle_1 |\varphi\rangle_2$ will arrive at

$$\begin{aligned} |\phi\rangle_q |\psi\rangle_1 |\varphi\rangle_2 \longrightarrow & \frac{1}{\sqrt{2}}|g\rangle (\gamma |\varphi\rangle_1 |\psi\rangle_2 - \eta |\psi\rangle_1 |\varphi\rangle_2) \\ & + \frac{1}{\sqrt{2}}|e\rangle (\gamma |\varphi\rangle_1 |\psi\rangle_2 + \eta |\psi\rangle_1 |\varphi\rangle_2). \end{aligned} \quad (15)$$

Now let's perform the von Neumann measurement on the flux qubit with respect to the basis $\{|g\rangle, |e\rangle\}$, one can immediately find that the probability collapsing on the state $|g\rangle$ is given by

$$p_g = \frac{1}{2}[1 - (\gamma^*\eta + \gamma\eta^*)F^2] \quad (16)$$

with $F = |\langle\varphi|\psi\rangle|$ denoting the fidelity between the two states. Thus for any nonvanishing $\gamma^*\eta + \gamma\eta^*$ known beforehand, one can easily find the fidelity of the two states of the two memories by the measurement probability.

In fact, the above procedure can also be used to determine the entanglement that we have prepared in the above section. As usual, to prepare entanglement, one has to prepare the initial state like $|\phi\rangle_q |\psi\rangle_1 |\varphi\rangle_2$. Since all the information of the initial state is known, one can calculate the entanglement by some proper entanglement measure such as the concurrence [81] defined by

$$C(|\psi_{\pm}\rangle) = \sqrt{2[1 - \text{Tr}(\rho_r^2)]} \quad (17)$$

with ρ_r representing the reduced density matrix of the state $|\psi_{\pm}\rangle$. Here, we would like to emphasize that actually this concurrence can be measured directly based on the above experimental procedure. In particular, if we *don't know the initial states* in which the two memories are, one can find that the entanglement prepared through the above procedure can also be directly measured. To see this, let's substitute the state $|\psi_{\pm}\rangle$ into Eq. (17). One can immediately find that

$$C(|\psi_{\pm}\rangle) = \sqrt{2 - \frac{1}{2}\{|\gamma|^4 + |\eta|^4 + 2[2|\gamma|^2|\eta|^2 \pm (\gamma\eta^* + \gamma^*\eta)]F^2 + (\gamma^2\eta^{*2} + \gamma^{*2}\eta^2)F^4\}}. \quad (18)$$

It is obvious that F^2 in Eq. (18) can be measured based on the measurement of the fidelity given by Eq. (16), since γ and η are known beforehand.

Experimental feasibility—Recent experiments have achieved arbitrary control of a single superconducting resonator in circuit QED [82–84]. For instance, [82] experimentally generated Fock states in a superconducting resonator by coupling a tunable superconducting qubit, [83] demonstrated the preparation of arbitrary quantum states of a single resonator, [84] experimentally created a superposition of coherent states (i.e., a cat state) of a resonator, and [85] experimentally implemented a universal set of gates on a qubit encoded into a resonator using the cat-code. Here we will take the preparation of entanglement as examples to give a necessary

analysis on the feasibility of our scheme. For an experimental implementation, we consider the qubit-memory system initially state is

$$(i) |\phi\rangle_q |N\rangle_1 |0\rangle_2, \quad (19)$$

$$(ii) |\phi\rangle_q |\alpha\rangle_1 |-\beta\rangle_2, \quad (20)$$

$$(iii) |\phi\rangle_q |\psi_e\rangle_1 |\varphi_o\rangle_2, \quad (21)$$

where $|\phi\rangle_q = \frac{1}{\sqrt{2}}(|g\rangle + |e\rangle)$ (i.e., $\gamma = \eta = \frac{1}{\sqrt{2}}$), $|\psi_e\rangle_1 = N_e(|\alpha\rangle_1 + |-\alpha\rangle_1)$, and $|\varphi_o\rangle_2 = N_o(|\beta\rangle_2 - |-\beta\rangle_2)$. Here, $|\alpha\rangle_1$ and $|\beta\rangle_2$ ($|-\alpha\rangle_1$ and $|-\beta\rangle_2$) are coherent states of two memories 1 and 2, $N_e = \frac{1}{\sqrt{2}}[1 + \exp(-2\alpha^2)]^{-1/2}$ and $N_o = \frac{1}{\sqrt{2}}[1 - \exp(-2\beta^2)]^{-1/2}$ are normalization factors.

For a flux qubit, the transition frequency between two neighbor levels is typically 1 to 20 GHz. Thus, the $|a\rangle \leftrightarrow |e\rangle$ transition frequency of flux qubit can be highly detuned from the resonator frequency. Accordingly, the coupling effect of the resonator with the $|a\rangle \leftrightarrow |e\rangle$ transition is negligibly small, which is thus not considered in the numerical simulation for simplicity.

When the dissipation and the dephasing are included, the dynamics of the lossy system is determined by the following Lindblad master equation

$$\begin{aligned} \frac{d\rho}{dt} &= -i[H_{I,k}, \rho] + \sum_{i=1,2} \kappa_i \mathcal{L}[a_i] \\ &+ \gamma_{ag} \mathcal{L}[\sigma_{ag}^-] + \gamma_{ea} \mathcal{L}[\sigma_{ea}^-] + \gamma_{eg} \mathcal{L}[\sigma_{eg}^-] \\ &+ \sum_{j=a,e} \{\gamma_{\varphi j} (\sigma_{jj} \rho \sigma_{jj} - \sigma_{jj} \rho / 2 - \rho \sigma_{jj} / 2)\}, \end{aligned} \quad (22)$$

where $H_{I,k}$ is either $H_{I,1}$ or $H_{I,2}$, i represents quantum memory (i.e., resonator or NV ensemble) i ($i = 1, 2$), $\sigma_{ag}^- = |g\rangle \langle a|$, $\sigma_{ea}^- = |a\rangle \langle e|$, $\sigma_{eg}^- = |g\rangle \langle e|$, $\sigma_{jj} = |j\rangle \langle j|$ ($j = a, e$); and $\mathcal{L}[\Lambda] = \Lambda \rho \Lambda^\dagger - \Lambda^\dagger \Lambda \rho / 2 - \rho \Lambda^\dagger \Lambda / 2$, with $\Lambda = a_i, \sigma_{ag}^-, \sigma_{ea}^-, \sigma_{eg}^-$. Here, κ_i is the decay rates of quantum memory i ($i = 1, 2$). In addition, γ_{ag} is the energy relaxation rate of the level $|a\rangle$ of qubit, γ_{ea} (γ_{eg}) is the energy relaxation rate of the level $|e\rangle$ of qubit for the decay path $|e\rangle \rightarrow |a\rangle$ ($|g\rangle$), and $\gamma_{\varphi j}$ is the dephasing rate of the level $|j\rangle$ of qubit ($j = a, e$).

The fidelity of the operation takes the form $\mathcal{F} = \sqrt{\langle \psi_{id} | \rho | \psi_{id} \rangle}$, where $|\psi_{id}\rangle$ is the output state of an ideal system (i.e., without dissipation and dephasing) and ρ is the final density operator of the system when the operation is performed in a realistic situation. Here, the output state $|\psi_{id}\rangle$ is given by $\frac{1}{\sqrt{2}}(|\psi_+\rangle|e\rangle + |\psi_-\rangle|g\rangle)$. Based on Eqs. (19)-(21), the ideal entangled state of two quantum memories is

$$(i) |N\rangle_1 |0\rangle_2 \pm |0\rangle_1 |N\rangle_2, \quad (23)$$

$$(ii) |\alpha\rangle_1 |-\beta\rangle_2 \pm |-\beta\rangle_1 |\alpha\rangle_2, \quad (24)$$

$$(iii) |\psi_e\rangle_1 |\varphi_o\rangle_2 \pm |\varphi_o\rangle_1 |\psi_e\rangle_2. \quad (25)$$

By solving the master equation (22), the fidelity of the entangled state generation can be calculated for Eqs. (23)-(25), respectively. We now numerically calculate the fidelity for the operation. We choose resonator-qubit or NV ensemble-qubit coupling constants $g/2\pi = 70$ MHz. The values of g here are available in experiments because the resonator-qubit and the NV ensemble-qubit coupling strengths are approximately 636 MHz [18] and 70 MHz [23] reported in experiments. In addition, we set $k=1$, $N = 5$, $\alpha = \beta = 1.1$, $\Omega/2\pi = 100$ MHz (attainable in experiments [86, 87]), $\gamma_{j,\varphi e}^{-1} = \gamma_{j,\varphi f}^{-1} = 2 \mu s$, and $\gamma_{eg}^{-1} = \gamma_{fe}^{-1} = \gamma_{fg}^{-1} = 5 \mu s$. Here we consider a rather conservative case for the decoherence times of flux qubit [88, 89]. Furthermore, one sets the lifetimes of two quantum memories (i.e., resonators or NV ensembles) $\kappa_1^{-1} = \kappa_2^{-1} = 5 \mu s$, which are also conservative estimate compared with those reported in experiments [29, 90, 91].

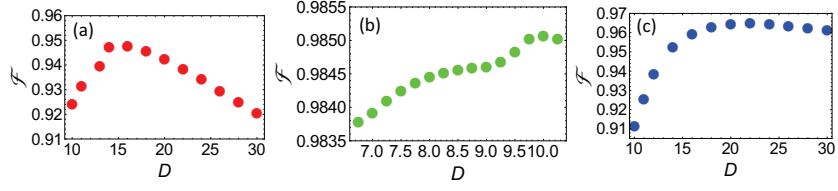


Fig. 3. Fidelity \mathcal{F} versus $D = \delta/g$. (a) Fidelity versus D for NOON states. (b) Fidelity versus D for entangled coherent states. (c) Fidelity versus D for entangled cat states. The parameters used in the numerical simulation are referred in the text.

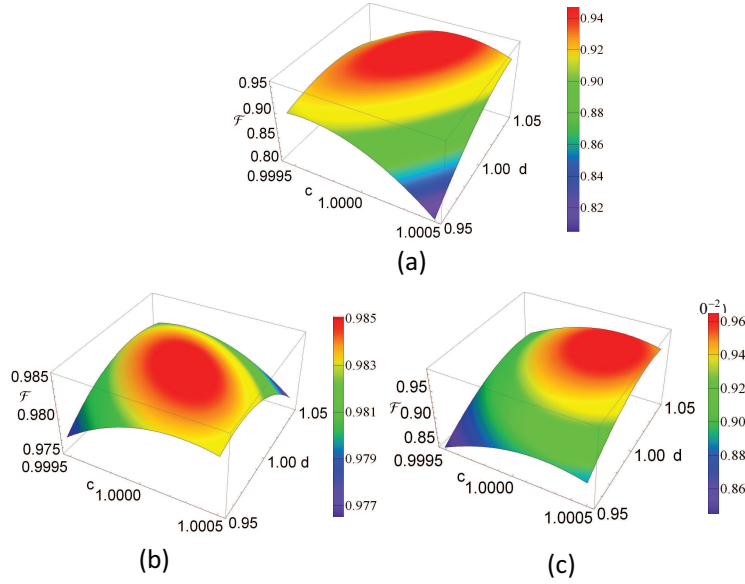


Fig. 4. Fidelity versus c and d , which are plotted by choosing (a) $D = 16$, (b) $D = 10$, and (c) $D = 22$, respectively.

Figure 3 shows the fidelity versus $D = \delta/g$, which are plotted for the (i) NOON states [Eq. (23)], (ii) entangled coherent states [Eq. (24)], (iii) entangled cat states [Eq. (25)], respectively. From Figs. 3(a)-3(c), one can obtain that a high fidelity 96.0%, 98.5% and 96.5% for $D = 16, 10$ and 22 , respectively. In the following analysis, we will choose $D = 16, 10$ and 22 for the cases of (i) (ii) and (iii), respectively. For $D = 16, 10$ and 22 , one has the resonator-qubit or NV ensemble-qubit frequency detunings $\delta/2\pi = 1.12$ GHz, 0.7 GHz and 1.54 GHz. The numerical simulation shows that the high-fidelity generation of above entangled states of two quantum memories is feasible with the state-of-the-art circuit QED technology.

In a realistic situation, the inhomogeneous broadening of quantum memories may induce the inhomogeneous memory-qubit coupling and unequal memory-qubit frequency detuning. Thus, we numerically calculate the fidelity by setting $\delta_1/2\pi = \delta$, $\delta_2/2\pi = c\delta$, $g_1 = g$, and $g_2 = dg$, with $c \in [0.9995, 1.0005]$ and $d \in [0.95, 1.05]$. The other parameters used in the numerical simulation for Fig. 4 are the same as those used in Fig. 3. Figures 4(a)-4(c) display the fidelity versus c and d , which are plotted by choosing $D = 16, 10$ and 22 , respectively. Figure 4(a) shows that for $c \in [0.9995, 1.0003]$ and $d \in [0.98, 1.05]$, the fidelity can be greater than 90%.

As illustrated in Fig. 4(b), the effect of the inhomogeneous broadening on the fidelity is very small with $c \in [0.9995, 1.0005]$ and $d \in [0.95, 1.05]$. Figure 4(c) displays that the fidelity is greater than 92% for $c \in [0.9998, 1.0005]$ and $d \in [0.97, 1.05]$. From Fig. 4, one can see that the high-fidelity generation of entangled states of two quantum memories can be achieved for small errors in memory-qubit coupling and detuning.

4. Conclusion

We have proposed a method to implementing a hybrid Fredkin gate between a single superconducting flux qubit and two resonators or NV ensembles in any discrete-variable or continuous-variable states. Due to the usage of only one single three-level qubit, the experimental setup is simplified and the experimental difficulty is greatly reduced. In addition, the protocol requires only a single unitary operation, thus the operation procedure is greatly simplified. The proposal can also be applied to other kinds of superconducting qubits (e.g., superconducting charge qubits, transmon qubits, Xmon qubits, phase qubits) coupled to two 1D resonators or two 3D cavities. Furthermore, our scheme can be used to generate arbitrary entangled states of two quantum memories, such as NOON states, entangled coherent states, and entangled cat states. It is also shown that our scheme can be used to measure the fidelity and entanglement between the two memories. Numerical simulation shows that these entangled states can be high-fidelity created with circuit QED of the existing technology.

Finally, we would like to emphasize that our scheme can also be used to realize a controlled-shift operation with a qudit as a control state. If the control qudit includes two particular energy levels $|up\rangle$ and $|down\rangle$ with the transition frequency much less than the other pairs of energy levels, the two target memories will swap their states conditioned on the control state $|down\rangle$. Similarly, if the highest energy level is much farther off resonant with the other energy levels, one could use the other energy levels as a whole to control the swapping of the states of the two memories. All the realizations need us to carefully choose the various parameters covered in the system. It should be noted that the introduction of the multiple energy levels usually lead to the complex undesired couplings which could be small to some good approximation, but could be a little larger than the case of less energy levels under the same condition. All the above can be easily demonstrated following the similar procedures as our main text. Our finding provides a new way for realizing the Fredkin gate or quantum entanglement between two quantum memories, which may have many potential applications in quantum information processing based on circuit QED.

Funding

National Natural Science Foundation of China (NSFC) (11775040, 11375036); Xinghai Scholar Cultivation Plan.